

Supporting Information

UV-induced Photolysis of Polyurethanes

Charlotte Petit, ^{a‡} Julian Bachmann, ^{ab‡} Lukas F. Michalek, ^a Yohann Catel, ^c Eva Blasco, ^d
James Blinco, ^{*a} Andreas-N. Unterreiner, ^{*b} Christopher Barner-Kowollik ^{*ae}

^aCentre for Materials Science, School of Chemistry and Physics, Queensland University of
Technology (QUT), 2 George Street, Brisbane, QLD 4000, Australia.

E-Mails: christopher.barnerkowollik@qut.edu.au, j.blinco@qut.edu.au

^bInstitute of Physical Chemistry, Karlsruhe Institute of Technology (KIT), Fritz-Haber-Weg 2,
76131 Karlsruhe, Germany. E-Mail: andreas.unterreiner@kit.edu

^cIvoclar Vivadent AG, Bendererstrasse 2, 9494 Schaan, Liechtenstein

^dInstitute of Nanotechnology (INT), Karlsruhe Institute of Technology (KIT), Hermann-von-
Helmholtz-Platz 1, 76344 Eggenstein-Leopoldshafen, Germany; Institute of Organic
Chemistry, Heidelberg University, Im Neuenheimer Feld 270; Center for Advanced Materials,
Heidelberg University, Im Neuenheimer Feld 225, 69120 Heidelberg, Germany

^eCentre for a Waste-Free World, Queensland University of Technology (QUT), 2 George
Street, Brisbane, QLD 4000, Australia. E-Mail: christopher.barnerkowollik@qut.edu.au

[‡] *These authors contributed equally*

Contents

1. EXPERIMENTAL SECTION	1
1.1. Materials	1
1.2. Characterization methods	1
1.3. Synthesis of <i>Tert</i> -butyl 2-(4-acetyl-2-methoxyphenoxy)acetate, 2	9
1.4. Synthesis of 2-(4-acetyl-2-methoxy-5-nitrophenoxy)acetic acid, 3	12
1.5. Synthesis of 1-(4-(2-hydroxyethoxy)-5-methoxy-2-nitrophenyl)ethan-1-ol, 4	15
2. ANALYSIS.....	20
2.1. Evolution of physicooptical properties of precursors and <i>o</i> NB-dialcohol	20
2.2. Proof of degradation of the <i>o</i> NB dialcohol, 4.....	21
2.3. Degradation of kinetics with LED irradiation.....	22
2.4. EPR of 4 under light irradiation	27
2.5. Action Plot of 4	29
2.6. Deconvolution of step-growth generated PU polymers	31
2.7. PLD-SEC of step growth generated PU polymers	32
2.8. SEC-ESI- MS of PUs.....	35

1. EXPERIMENTAL SECTION

1.1. Materials

The following chemicals were used as received without further purification.

4'-Hydroxy-3'-methoxyacetophenone (98%, Sigma Aldrich), *tert*-butyl bromoacetate (98%, Alfa Aesar), potassium carbonate (99%, Chem-Supply), nitric acid (70%, AIM Scientific), acetic anhydride (99%, Chem-Supply), borane tetrahydrofuran complex solution (1.0 M in THF, Sigma Aldrich), hexamethylene diisocyanate (HDI, >98%, Sigma Aldrich), dibutyltin dilaurate (DBTL, 95%, Sigma Aldrich), amberlite® IRA743 (free base, Sigma-Aldrich).

Solvents: Acetonitrile (AcN, HPLC Grade, Fisher), ethyl acetate (EA, Analytical reagent, Fisher), dichloromethane (DCM, analytical reagent, Fisher), ethanol (EtOH, analytical reagent, Ajax Finechem), acetonitrile-d₃ (AcN, 99.8%D, Cambridge Isotope Laboratories), dimethylsulfoxide-d₆ (DMSO, 99.9%D, Cambridge Isotope Laboratories), Tetrahydrofuran (THF, HPLC grade, Fisher).

1.2. Characterization methods

LC-ESI-MS LC-MS measurements were performed on an UltiMate 3000 UHPLC System (Dionex, Sunnyvale, CA, USA) consisting of a pump (LPG 3400SZ), autosampler (WPS 3000TSL) and a temperature controlled column compartment (TCC 3000). Separation was performed on a C18 HPLC column (Phenomenex Luna 5 μ m, 100 Å, 250 \times 2.0 mm) operating at 40 °C. Water (containing 5 mmol L⁻¹ ammonium acetate) and acetonitrile were used as eluents. A gradient of acetonitrile:H₂O 5:95 to 100:0 (v/v) in 7 min at a flow rate of 0.40 mL·min⁻¹ was applied. The flow was split in a 9:1 ratio, where 90 % of the eluent was directed through a DAD UV-detector (VWD 3400, Dionex) and 10 % was infused into the electrospray source. Spectra were recorded on an LTQ Orbitrap Elite mass spectrometer (Thermo Fisher Scientific, San Jose, CA, USA) equipped with a HESI II probe. The instrument was calibrated in the m/z range 74-

1822 using premixed calibration solutions (Thermo Scientific). A constant spray voltage of 3.5 kV, a dimensionless sheath gas and a dimensionless auxiliary gas flow rate of 5 and 2 were applied, respectively. The capillary temperature and was set to 300 °C, the S-lens RF level was set to 68, and the aux gas heater temperature was set to 100 °C.

Size-Exclusion Chromatography hyphenated Electrospray Ionisation Mass Spectrometry

(SEC-ESI-MS) Spectra were recorded on a Q Exactive Plus (Orbitrap) mass spectrometer (Thermo Fisher Scientific, San Jose, CA, USA) equipped with an HESI II probe. The instrument was calibrated in the m/z range 74-1822 using premixed calibration solutions (Thermo Scientific) and for the high mass mode in the m/z range of 600-8000 using ammonium hexafluorophosphate solution. A constant spray voltage of 3.5 kV, a dimensionless sheath gas and a dimensionless auxiliary gas flow rate of 10 and 0 were applied, respectively. The capillary temperature and was set to 320 °C, the S-lens RF level was set to 150, and the aux gas heater temperature was set to 125 °C. The Q Exactive was coupled to an UltiMate 3000 UHPLC System (Dionex, Sunnyvale, CA, USA) consisting of a pump (LPG 3400SD), autosampler (WPS 3000TSL), and a temperature-controlled column compartment (TCC 3000). Separation was performed on two mixed bed size exclusion chromatography columns (Agilent, Mesopore 250 × 4.6 mm, particle diameter 3 μm) with a precolumn (Mesopore 50 × 7.5 mm) operating at 30 °C. THF at a flow rate of 0.30 mL·min⁻¹ was used as eluent. The mass spectrometer was coupled to the column in parallel to an UV detector (VWD 3400, Dionex), and a RI-detector (RefractoMax520, ERC, Japan) in a setup described earlier.^[1] 0.27 mL·min⁻¹ of the eluent were directed through the UV and RI-detector and 30 μL·min⁻¹ were infused into the electrospray source after post-column addition of a 50 μM solution of sodium iodide in methanol at 20 μL·min⁻¹ by a micro-flow HPLC syringe pump (Teledyne ISCO, Model 100DM). A 100 μL aliquot of a polymer solution with a concentration of 2 mg·mL⁻¹ was injected into the SEC system.

Size Exclusion Chromatography (SEC) SEC elugrams were recorded on a system consisting of a 1515 Isocratic HPLC Pump, 2414 RI detector and a 717 Plus autosampler (Waters, Milford, USA), and a column set (PSS, Mainz, Germany) consisting of a guard column (50 × 8 mm, 10 μm) and two 1000 Å GRAM columns (300 × 8 mm, 10 μm). The eluent was HPLC grade THF. All molar mass data is reported relative to polystyrene standards (EasyCal, Agilent, Santa Clara, USA).

Nuclear Magnetic Resonance (NMR) Spectroscopy ¹H and ¹³C-NMR spectra were recorded on a Bruker System 600 Ascend LH, equipped with a BBO-Probe (5 mm) with z-gradient (¹H: 600.13 MHz, ¹³C 150.90 MHz). Resonances are reported in parts per million (ppm) relative to tetramethylsilane (TMS). The δ-scale was calibrated to the respective solvent signal of CHCl₃, DMSO-d₆ or Acetonitrile-d₃ for ¹H spectra and for ¹³C spectra on the middle signal of the CDCl₃ triplet, the DMSO quintet or the Acetonitrile septet. To analyse the spectra, the software MES-TRENOVA 11.0 was used. The resonances are quoted as follows: s = singlet, bs = broad singlet, d = doublet, t = triplet, q = quartet, quin = quintet, dd = doublet of doublets and m = multiplet.

Stationary UV/Vis Spectroscopy UV-Vis spectra were recorded on a Shimadzu UV-2700 spectrophotometer equipped with a CPS-100 electronic temperature control cell positioner. Samples were prepared in acetonitrile with a stock solution concentration of 1 mg/mL and measured in Hellma Analytics quartz high precision cell cuvettes with a path length of 10 mm at 25°C.

Electron Paramagnetic Resonance Spectroscopy (EPR) EPR spectra were recorded on a MiniScope MS400 spectrometer (Magnettech GMBH, Berlin, Germany) using CDCl₃ as the solvent and capillary tubes for liquid handling. Data simulation was performed with the MATLAB 2018a software package (The Mathworks, Natick, MA, USA) and a custom plug-in published elsewhere.^[2]

Fourier-Transformed Infrared Spectroscopy (FT-IR): FT-IR spectra were recorded on a Nicolet iS50 FTIR spectrometer in ATR configuration.

Laser-based Irradiation Experiments The incident light used for laser experiments came from a Coherent Opolette 355 tuneable OPO operated at 340 nm with a full width half maximum of 7 ns and a repetition rate of 20 Hz (**Figure S1**). The emitted pulse which has a flat-top spatial profile, was expanded to 6mm diameter using focusing lenses and directed upwards using a prism. The beam was then centred on a glass laser vial which is positioned in a 6 mm diameter slot in a temperature-controlled sample holder. The energy transmitted through the sample holder was measured using a Coherent Energy Max PC power meter. Transmittance of the glass vial was screened throughout the visible spectrum (**Figure S2, Table S1**).^[3] The transmittance values used were obtained analogously to a method reported previously. The glass vials were cut at a height of 3 mm. Thus, the number of photons delivered into the sample solution can be determined more precisely, taking the wavelength-dependent transmittance into account. The precise photon count can be calculated by

$$n_p = \frac{E_0 \cdot k \cdot T_c(\lambda) \cdot \lambda}{N_A \cdot hc} \quad \text{eq. 1}$$

with E_0 being the Energy per pulse, k the number of pulses, $T_c(\lambda)$ the transmittance of the glass vial at a given wavelength λ , N_A the Avogadro constant and hc the Planck's constant-speed of light product.

Conversion X and Yield Y were calculated by comparing the integrals of oNB (**Figure S15**) in their respective 1H NMR spectra (**Figure S15**) according to eq. 2 and 3.

$$X = 1 - \frac{n_{t=0}}{n_t} \quad \text{eq. 2}$$

$$Y = \frac{n_{4',t} - n_{4',t=0}}{n_{4,t=0}} \quad \text{eq. 3}$$

Action plot studies were performed in triplets with the standard deviation as error bars.

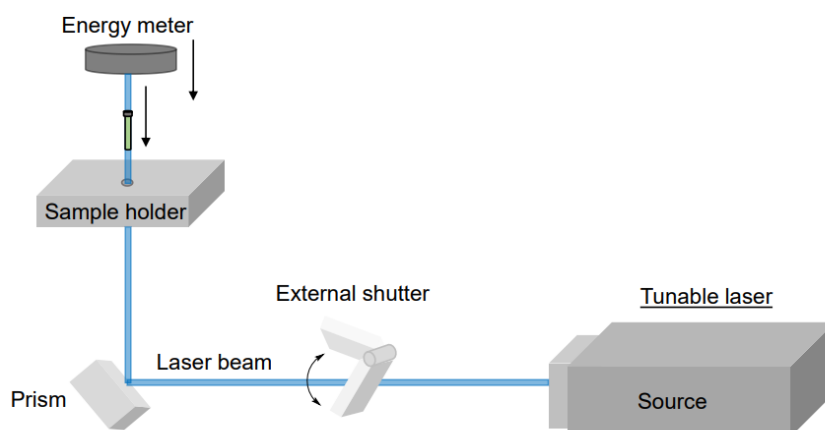


Figure S1: Experimental setup for the tunable laser experiments.

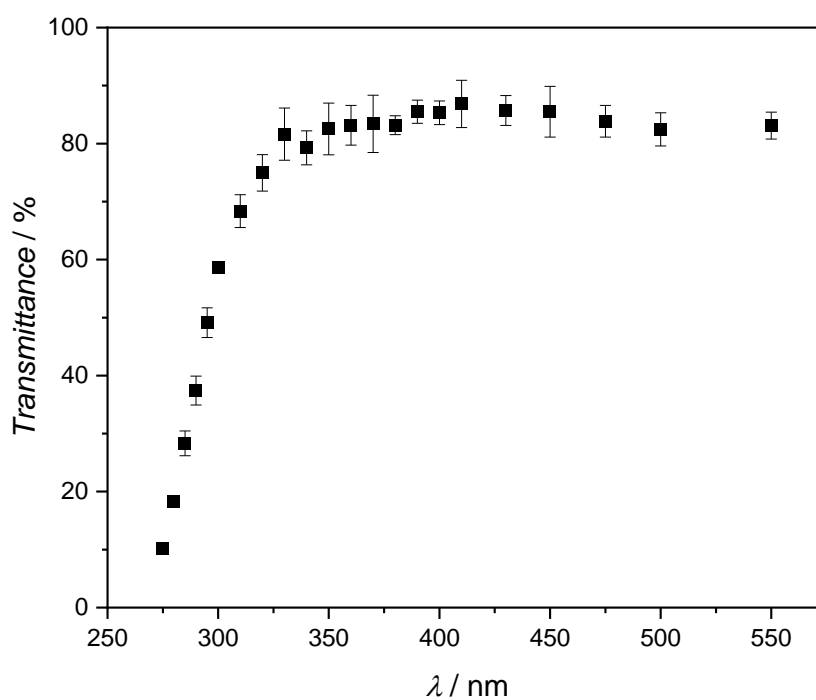
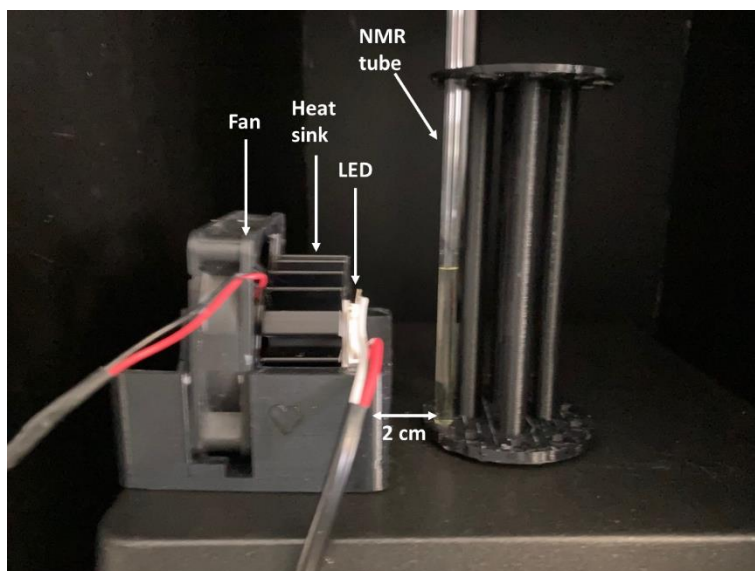


Figure S2: Transmittance of the used glass vial as a function of irradiation wavelength. Details are appended in **Table S1**.

Table S1: Wavelength-dependent transmittance values.

λ / nm	Transmittance / %	Δ Transmittance / %
275	10.23419	0.74982
280	18.25024	0.94703
285	28.31044	2.14137
290	37.43074	2.49132
295	49.11881	2.55629
300	58.57746	0.79725
310	68.34923	2.82282
320	74.95204	3.14492
330	81.62937	4.49571
340	79.27099	2.93382
350	82.52063	4.45387
360	83.15709	3.42489
370	83.40189	4.93431
380	83.17113	1.63659
390	85.48502	1.99615
400	85.31216	2.03069
410	86.83816	4.06669
430	85.71046	2.57226
450	85.49291	4.38069
475	83.84506	2.73637
500	82.44994	2.85985
550	83.10058	2.33119

LED-based Irradiation Experiments Irradiation experiments were performed using NMR tubes (for small molecule kinetics) and LEDs with an emission peak centred at 340, 365, 390 and 415 nm, respectively. The LEDs were powered using a tunable (Voltage U and current I) power supply. The LEDs were cooled with a fan placed directly behind the heat sink. Direct parameters for U , I and P_{calc} can be found at the respective chapter.



Scheme S1: Irradiation setup for kinetic experiments. The heat generated by the LED is dissipated by heat sink and fan. The NMR tube is placed in 2cm distance.

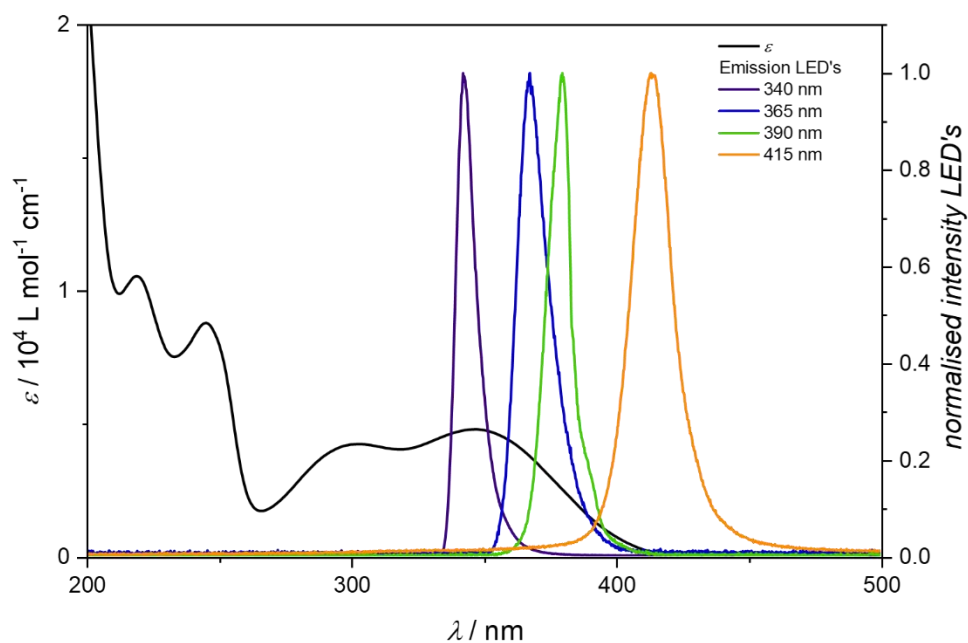


Figure S3: Emission spectra of the used LED's and the absorption spectrum of **4** in acetonitrile in comparison.

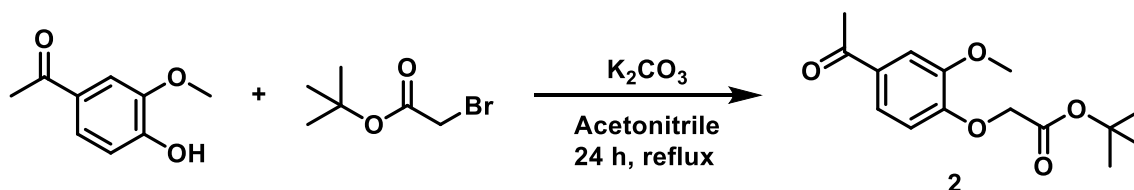
Quartz Crystal Microbalance (QCM) Measurements were performed using a Biolin Scientific QSense Explorer and window-module with 40 μ L volume above sensor and 250 μ L total volume. The temperature of the flow cell was kept at 25°C and a flow rate of 100 μ L \cdot min⁻¹ of milli-q water was employed. Each measurement was started by recording each sensors' fundamental frequency, recording a dry baseline for approximately 30min. Subsequently the flow cell was purged with milli-q water and a solvent baseline(<1Hz \cdot h⁻¹drift) was recorded for approximately 30min (without light). Finally, the sample was irradiated with a 365nm UV-LED to determine thin film degradation. Frequency was recorded until a stable state was reached.

X-ray photoelectron spectroscopy (XPS) Spectra were recorded on a KratosAxis Supra photoelectron spectrometer. During analysis, the charge compensation system was employed to prevent any localised charge build-up. For each sample, wide spectra and high-resolution spectra of individual peaks (N 1s) were recorded. All spectra were calibrated by setting the C 1s peak to 285.00eV. Evaluation, peak deconvolution, and fitting was carried out in Casa Software LtdCasaXPS 2.3.

The QCM sensors and glass slides were plasma cleaned prior to spin coating at 1500 rpm for 2 min using 10 μ L of a 7 μ g mL⁻¹ polymer solution.

Synthesis protocols were adapted from literature.^[4]

1.3. Synthesis of *Tert*-butyl 2-(4-acetyl-2-methoxyphenoxy)acetate, **2**



25.06 g acetovanillone (150.8 mmol, 1.20 eq.) and 59.15 g oven-dried K_2CO_3 (427.97 mmol, 3.42 eq.) were dispersed in 600 mL dry acetonitrile. After freeing the flask from oxygen by flushing with argon, 18.5 mL *tert*-butyl bromoacetate (24.44 g, 125.29 mmol, 1.00 eq) was added. The solution was stirred for 24 h under reflux. The mixture was filtered, and the solvent mostly removed under reduced pressure. The residual liquid was dispersed in 100 mL saturated $NaHCO_3$ solution and exposed to an ultrasonic bath for three minutes. The aqueous phase was extracted three times with 50 mL Et_2O . The organic solvent was mostly reduced under reduced pressure and washed once with 150 mL saturated $NaHCO_3$ solution. The organic solvent was completely evaporated obtaining **2** in pure colourless crystals. 34.29 g (98 % vs. theory)

1H -NMR, $DMSO-d_6$, 600 MHz, δ / ppm: 7.59 (d, 1H), 7.47 (dd, 1H), 6.94 (d, 1H), 4.77 (s, 2H), 3.83 (s, 3H), 2.54 (s, 3H), 1.42 (s, 9H)

^{13}C -NMR, $DMSO-d_6$, 600 MHz, δ / ppm: 196.45, 167.40, 151.34, 148.63, 130.51, 122.75, 112.10, 110.82, 81.63, 65.27, 55.66, 27.71, 26.40

LC-MS (ESI): m/z $[M+H]^+$, theo: 281.1384, exp: 281.1380, Δ / ppm: 1.42

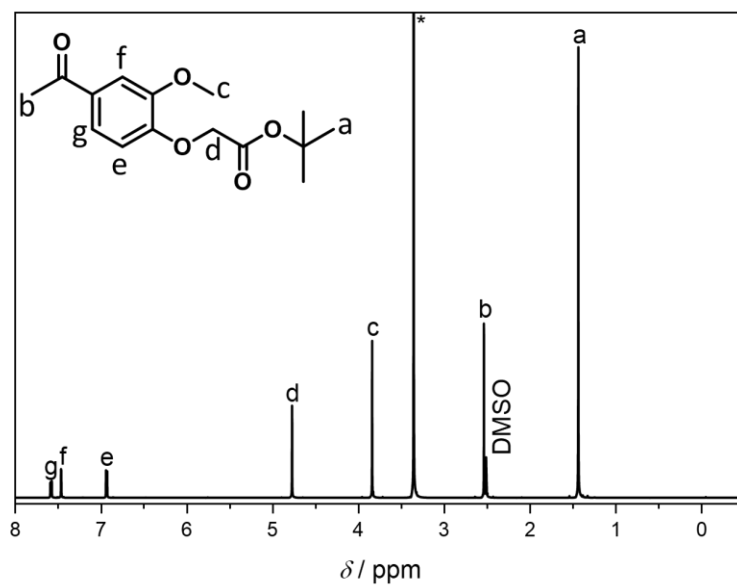


Figure S4: $^1\text{H-NMR}$ spectrum of **2** in DMSO-d_6 . * marks residual H_2O .

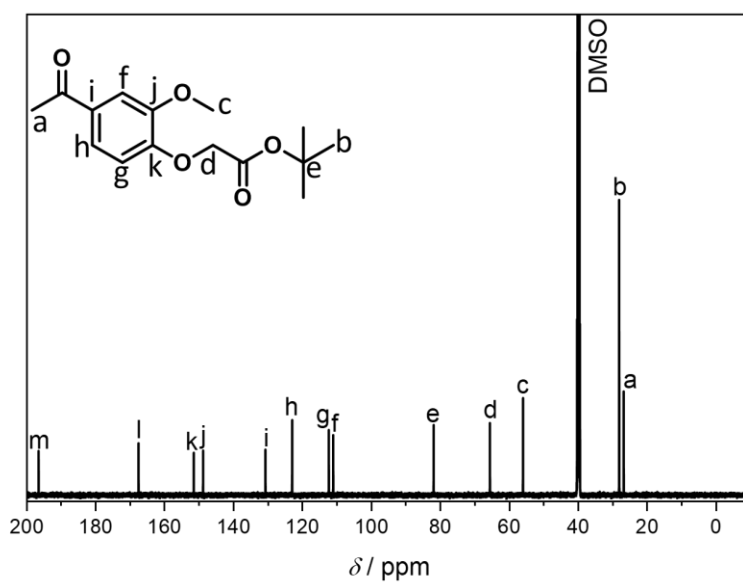


Figure S5: $^{13}\text{C-NMR}$ spectrum of **2** in DMSO-d_6 .

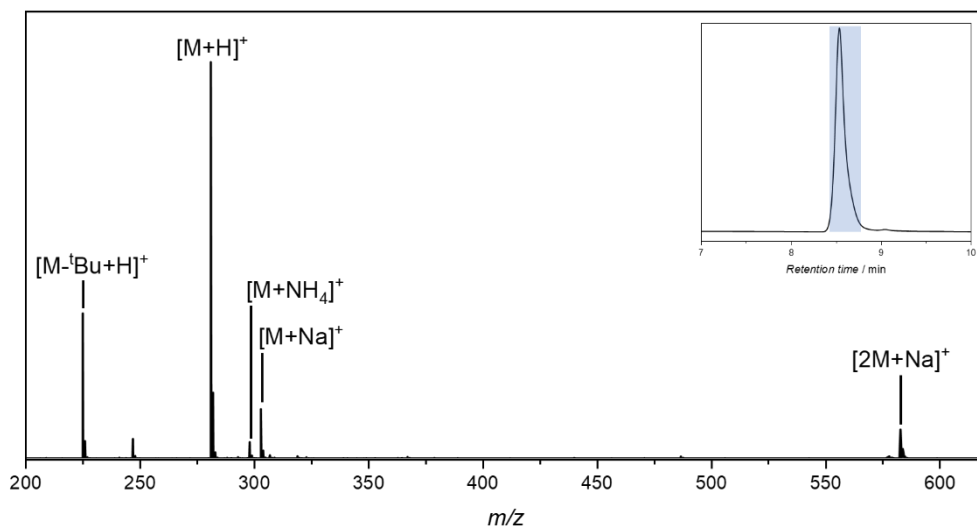
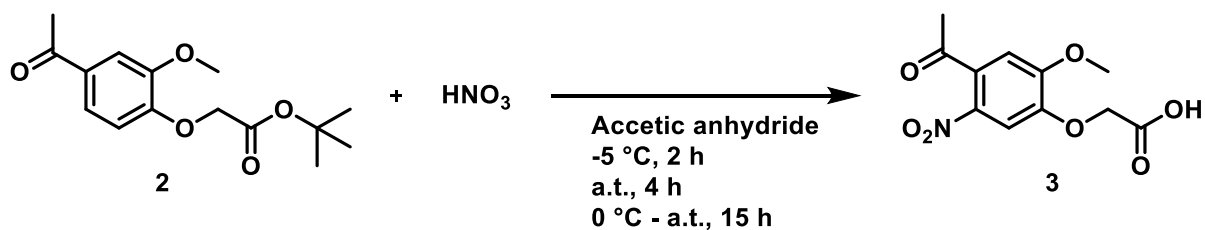


Figure S6: LC mass spectrum of **2**. The inlet (top right) shows the chromatogram (254 nm absorbance) between 7 and 10 minutes retention time. Area of the obtained mass spectrum is highlighted in blue.

Table S2: Detailed overview of found signals in the mass spectrum **Figure S6**, comparison with theoretically expected m/z values and derived error Δ .

Symbol	m/z_{exp}	m/z_{theo}	Δ / ppm	composition
$[2M+Na]^+$	583.2505	583.2514	1.54	$C_{30}H_{40}O_{10}Na_1^+$
$[M+Na]^+$	303.1199	303.1203	1.32	$C_{15}H_{20}O_5Na_1^+$
$[M+NH_4]^+$	298.1646	298.1649	1.01	$C_{15}H_{24}O_5N_1^+$
$[M+H]^+$	281.1384	281.1380	1.42	$C_{15}H_{21}O_5^+$
$[M-^tBu+H]^+$	225.0755	225.0757	0.89	$C_{11}H_{13}O_5^+$

1.4. Synthesis of 2-(4-acetyl-2-methoxy-5-nitrophenoxy)acetic acid, **3**



28 mL 70 % HNO_3 (439.5 mmol, 12.1 eq.) was added dropwise into 20 mL NaCl:Ice mixture cooled acetic anhydride (21.6 g, 211.6 mmol, 5.83 eq.) under rigorous stirring. A solution of previously grinded **2** (36.28 mmol, 1.0 eq., 10.1 g) in 30 mL acetic anhydride was added slowly into the stirring mixture dropwise at $-5\text{ }^\circ\text{C}$. The mixture was stirred at $-5\text{ }^\circ\text{C}$ for 2 h and subsequently at a.t. for 4 h. The mixture was poured into 300 mL crushed ice and allowed to reach a.t. overnight (15 h). The precipitate was filtrated and dried *in vacuo* at $40\text{ }^\circ\text{C}$ for 24 h. Product **3** was obtained in pale yellow amorphous solid. 5.77 g (59 % vs. theory).

$^1\text{H-NMR}$, DMSO- d_6 , 600 MHz, δ / ppm: 7.59 (s, 1H), 7.25 (s, 1H), 4.90 (s, 3H), 3.94 (s, 3H), 2.52 (s, 3H)

$^{13}\text{C-NMR}$, DMSO- d_6 , 600 MHz, δ / ppm: 199.34, 169.67, 153.30, 147.67, 138.00, 131.77, 110.12, 108.48, 65.21, 56.71, 30.06

LC-MS (ESI): m/z $[\text{M}+\text{H}]^+$, theo: 270.0608, exp: 270.0604, Δ / ppm: 1.48

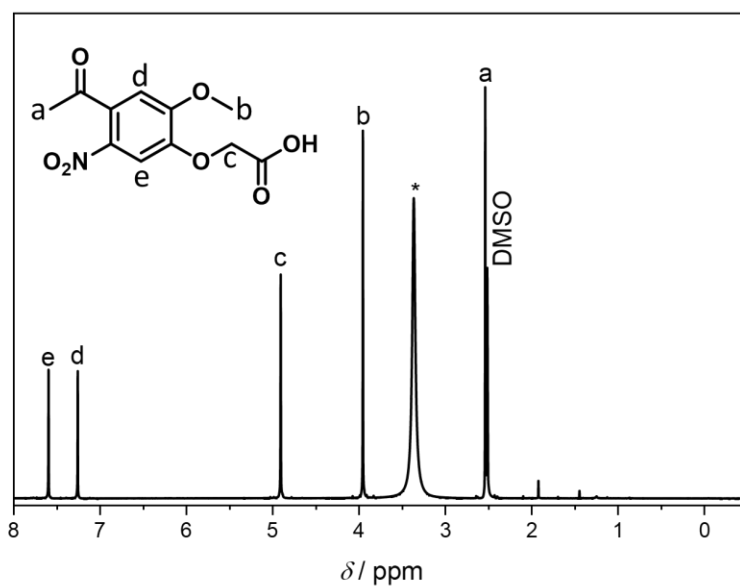


Figure S7: $^1\text{H-NMR}$ spectrum of **3** in DMSO-d_6 . * marks residual H_2O .

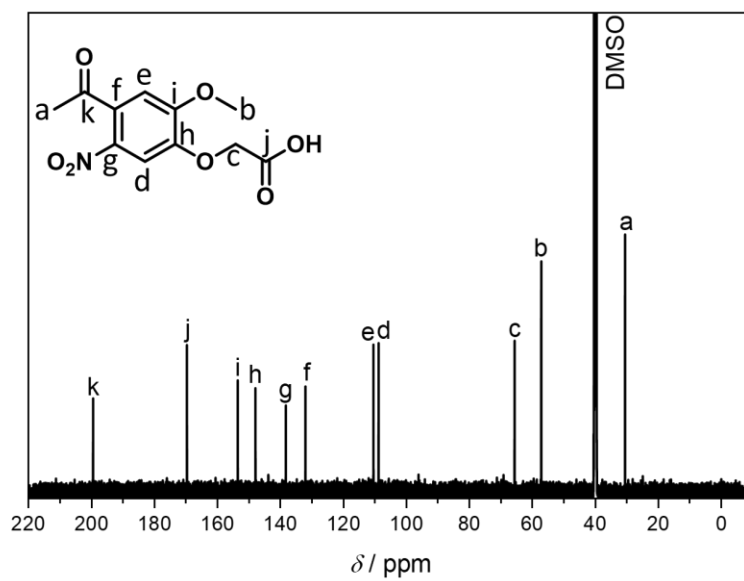


Figure S8: $^{13}\text{C-NMR}$ spectrum of **3** in DMSO-d_6 .

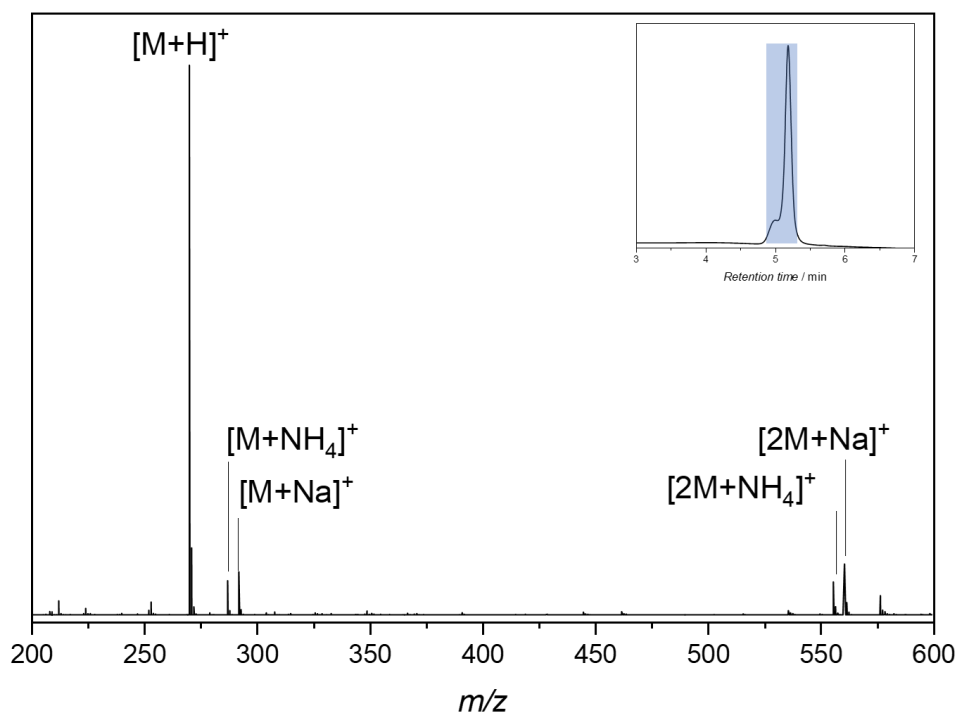
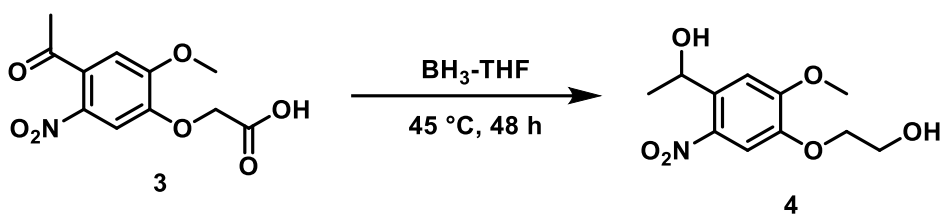


Figure S9: LC mass spectrum of **3**. The inlet (top right) shows the chromatogram (254 nm absorbance) between 3 and 7 minutes retention time. Area of the obtained mass spectrum is highlighted in blue.

Table S3: Detailed overview of found signals in the mass spectrum **Figure S9**, comparison with theoretically expected m/z values and derived error Δ .

Symbol	m/z_{exp}	m/z_{theo}	Δ / ppm	composition
$[2M+Na]^+$	561.0968	561.0963	0.89	$C_{22}H_{22}N_2O_{14}Na_1^+$
$[2M+NH_4]^+$	556.1410	556.1409	0.18	$C_{22}H_{26}N_3O_{14}^+$
$[M+Na]^+$	292.0428	292.0428	0.00	$C_{11}H_{11}N_1O_7Na_1^+$
$[M+NH_4]^+$	287.0874	287.0874	0.00	$C_{11}H_{15}N_2O_7^+$
$[M+H]^+$	270.0609	270.0608	0.37	$C_{11}H_{12}N_1O_7^+$

1.5. Synthesis of 1-(4-(2-hydroxyethoxy)-5-methoxy-2-nitrophenyl)ethan-1-ol, **4**



Under Schlenk conditions, 100 mL $\text{BH}_3\text{-THF}$ solution (100 mmol, 9.90 eq.) are added into a Schlenk flask containing 2.72 g (10.1 mmol, 1.00 eq.) of **3** while stirring via a transfer canula. The mixture was warmed up to $45\text{ }^\circ\text{C}$ and stirred at this temperature for 48 h. Afterwards, the reaction mixture was poured into an ice-cooled water:ethanol mixture (75:50 mL) and stirred for 5 minutes. After removing the solvent under reduced pressure, the solid residue was purified by submission to Ion-exchanging chromatography (Amberlite 743) and afterwards to chromatography (SiO_2 , $\text{Et}_2\text{O}/\text{EA}$, 85/15). Product **4** was obtained as a yellow amorphous solid. 1.91 g (73 % vs. theory).

$^1\text{H-NMR}$, DMSO-d_6 , 600 MHz, δ / ppm: 7.55 (s, 1H), 7.36 (1H), 5.47 (d, 1H), 5.26 (dq, 1H), 4.90 (t, 1H), 4.06 (t, 2H), 3.90 (s, 3H), 3.72 (q, 2H), 1.37 (d, 3H)

$^{13}\text{C-NMR}$, DMSO-d_6 , 600 MHz, δ / ppm: 153.41, 146.46, 138.89, 137.95, 109.07, 108.49, 70.75, 63.91, 59.36, 55.98, 25.17

LC-MS (ESI): m/z $[\text{M}+\text{NH}_4]^+$, theo: 275.1238, exp: 275.1239, Δ / ppm: 0.36

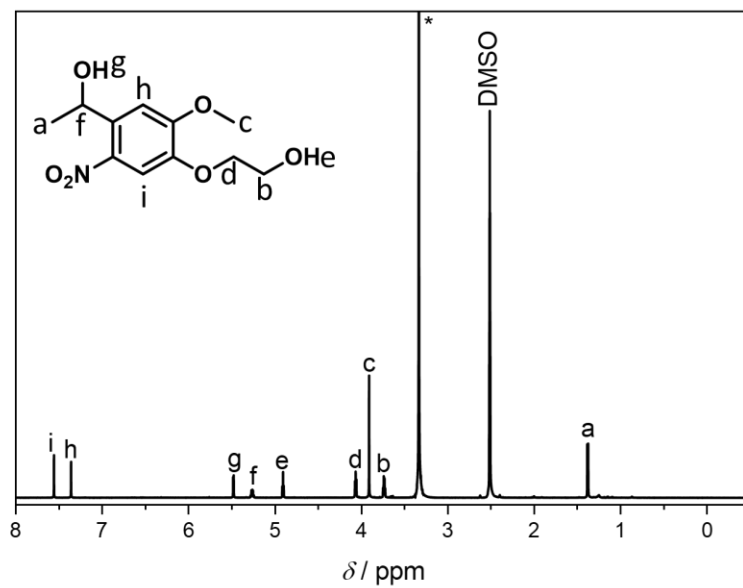


Figure S10: ¹H-NMR spectrum of **4** in DMSO-d₆. * marks residual H₂O

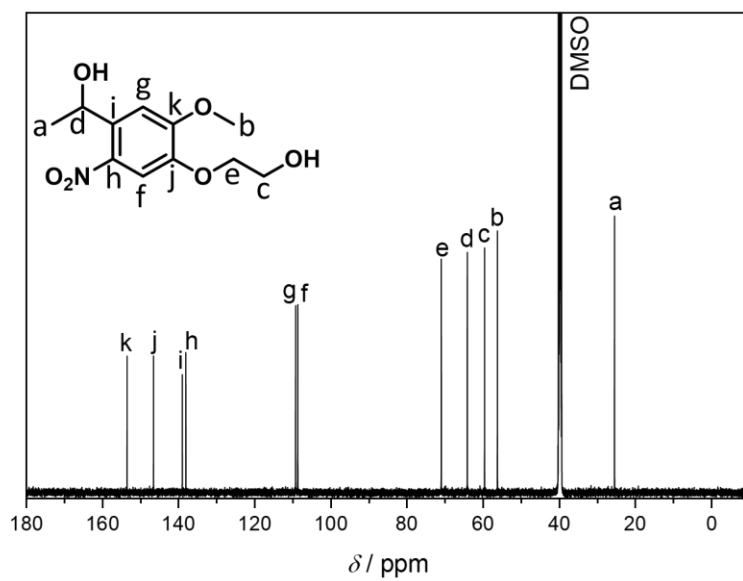


Figure S11: ¹³C-NMR spectrum of **4** in DMSO-d₆.

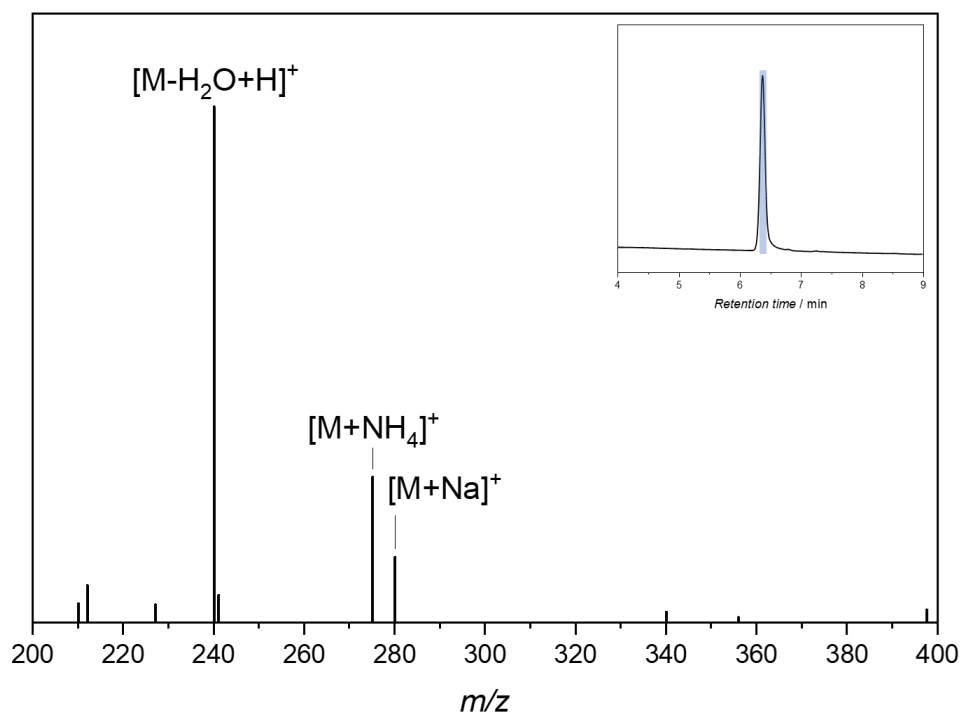
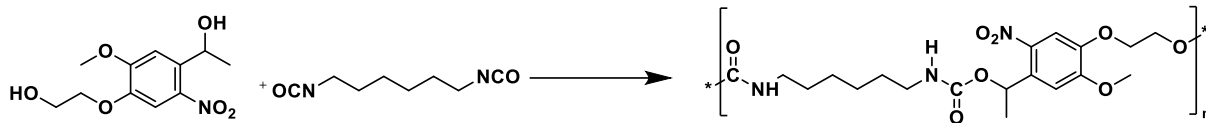


Figure S12: LC mass spectrum of **4**. The inlet (top right) shows the chromatogram (254 nm absorbance) between 4 and 9 minutes retention time. Area of the obtained mass spectrum is highlighted in blue.

Table S4: Detailed overview of found signals in the mass spectrum **Figure S12**, comparison with theoretically expected m/z values and derived error Δ .

Symbol	m/z_{exp}	m/z_{theo}	Δ / ppm	Composition
$[M+Na]^+$	280.0793	280.0792	0.36	$C_{11}H_{15}N_1O_6Na_1^+$
$[M+NH_4]^+$	275.1239	275.1238	0.36	$C_{11}H_{19}N_2O_6^+$
$[M-H_2O+H]^+$	240.0867	240.0866	0.42	$C_{11}H_{14}N_1O_5^+$

1.6. Synthesis of coPoly(oNB-dialcohol-*alt*-HDI),



In a crimped vial, 500 mg of *o*NB-diol (1 eq.) is solubilized in 2 mL of ethyl acetate in a sonication bath at 40 °C for 10min. A solution of 354 mg of 1,6-hexamethyl diisocyanate (1 eq.) and 405 μ L of dibutyltin dilaurate in 2 mL of EA is subsequently added to the vial. The reaction mixture was maintained at 70 °C for 2 to 20 min. After the determined time of reaction, ethyl acetate was added, the polymer filtered off and dried overnight at 40 °C under vacuum.

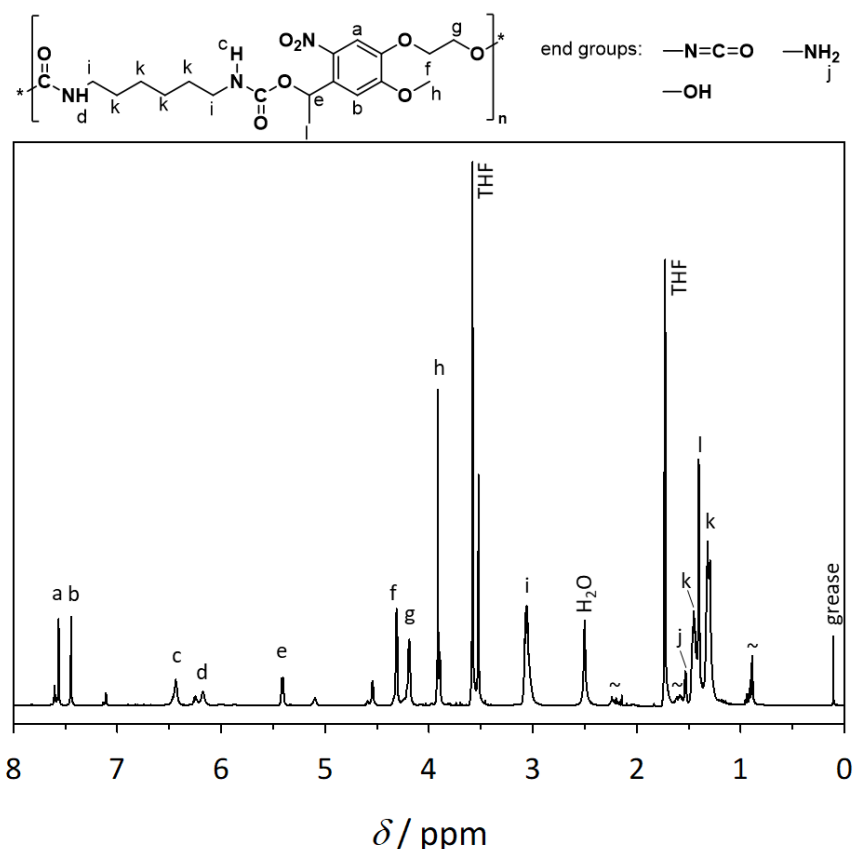


Figure S13. $^1\text{H-NMR}$ spectrum in THF-d₈ of polyurethane oligomers of *o*NB-dialcohol and hexamethyl diisocyanate obtained after 2 min reaction (refer to the Experimental section). ~ residual catalyst.

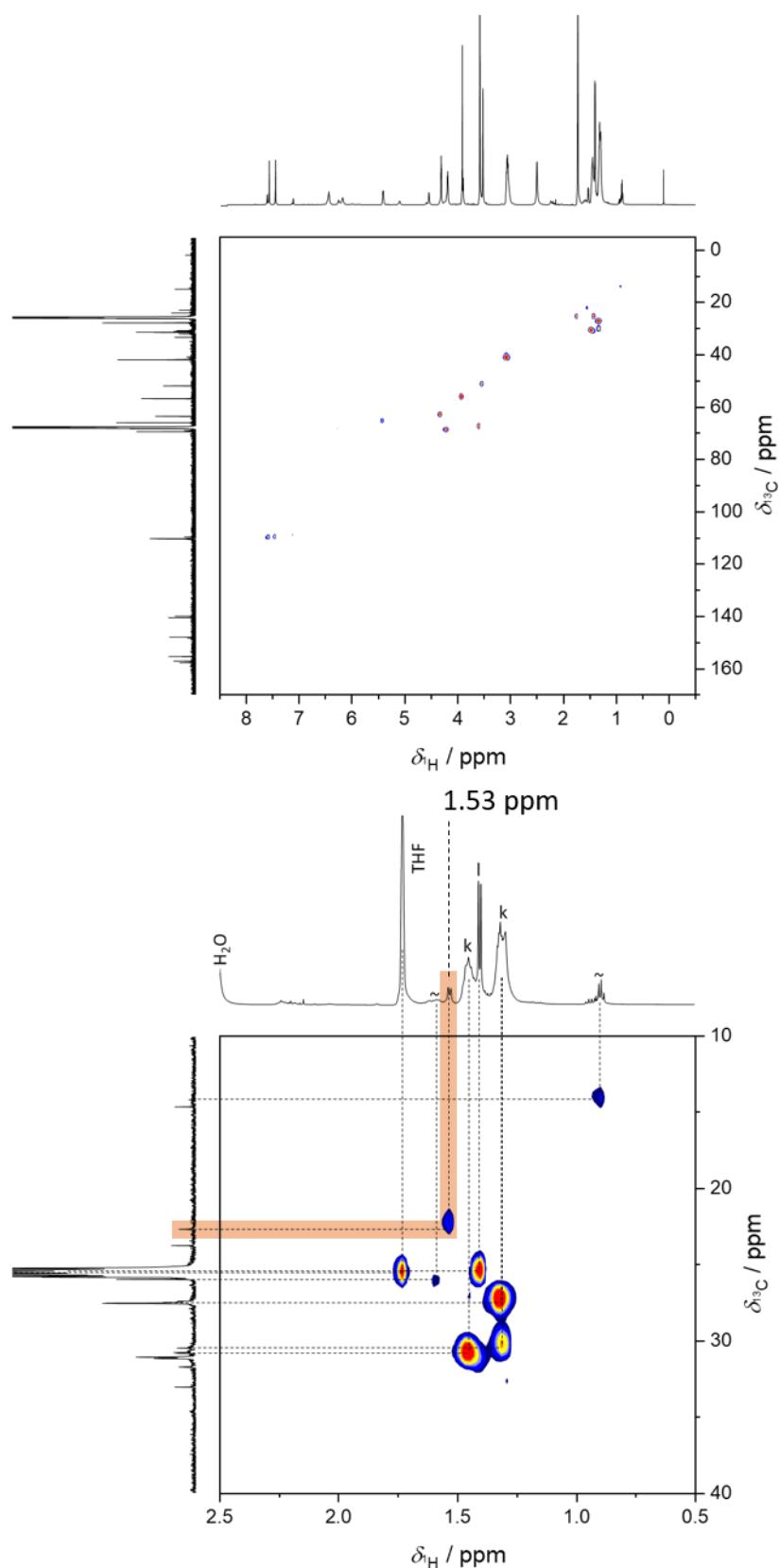
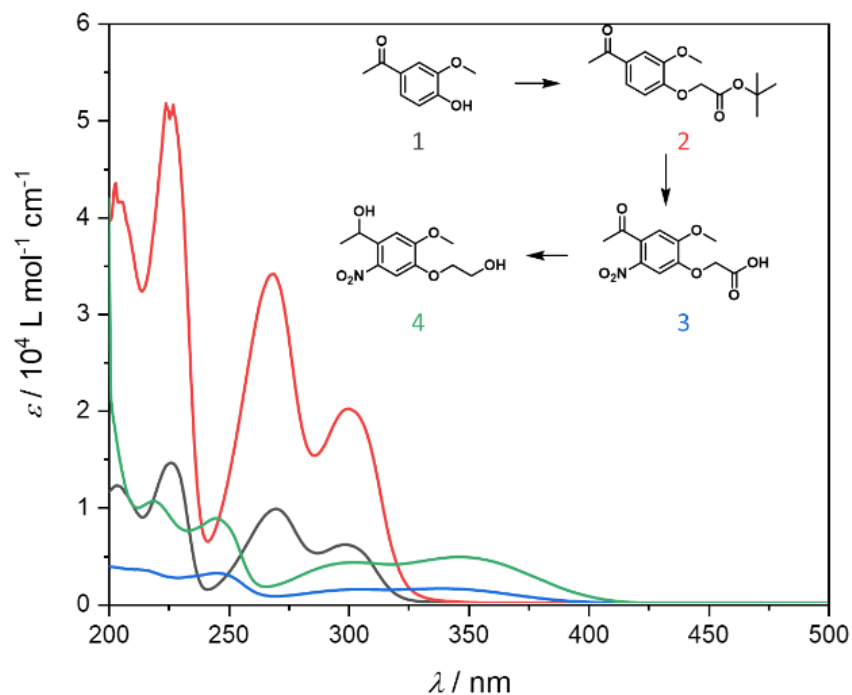


Figure S14. Top: Full HSQC-NMR spectrum of the 2 min cured polymer in THF-d₈. Bottom: Enlarged spectrum between 2.5 and 0.5 ppm. The ¹H NMR resonance at 1.53 ppm, suspected to be associated with the protons belonging to amine group, and its correlated ¹³C signal are highlighted in orange. ~ residual catalyst.

2. ANALYSIS

2.1. Evolution of physicooptical properties of precursors and *o*NB-dialcohol



Scheme S2: Ultraviolet-Visible absorbance spectra of the *o*NB-dialcohol and its intermediates, 1: Acetovanillone, 2: tert-butyl 2-(4-acetyl-2-methoxyphenoxy)acetate, 3: 2-(4-acetyl-2-methoxy-5-nitrophenoxy)acetic acid, 4: 1-(4-(2-hydroxyethoxy)-5-methoxy-2-nitrophenyl)ethan-1-ol

2.2. Proof of degradation of the *o*NB dialcohol, 4

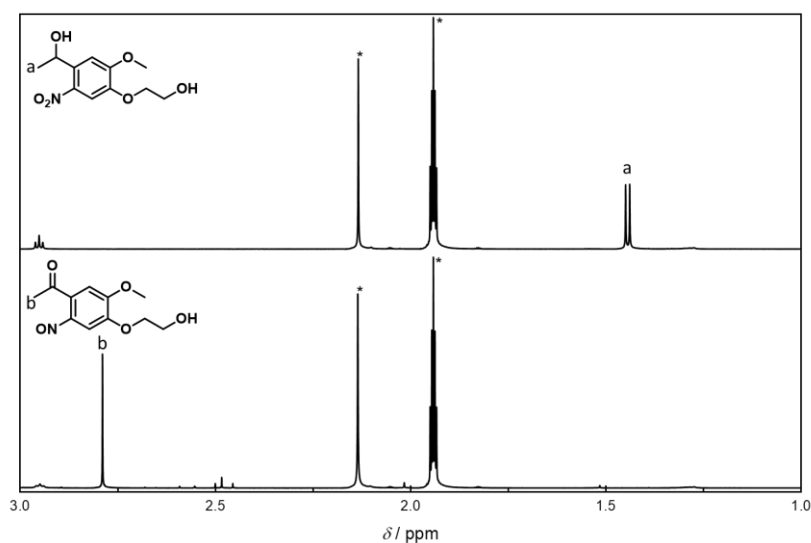


Figure S15: ¹H NMR spectra of the *o*NB dialcohol before (top, 4) and after (bottom, 4') UV-irradiation (365 nm LED, 60 minutes, Acetonitrile-d₃). The protons a and b belong to the methyl group in alpha position of the secondary alcohol and carbonyl group, respectively.

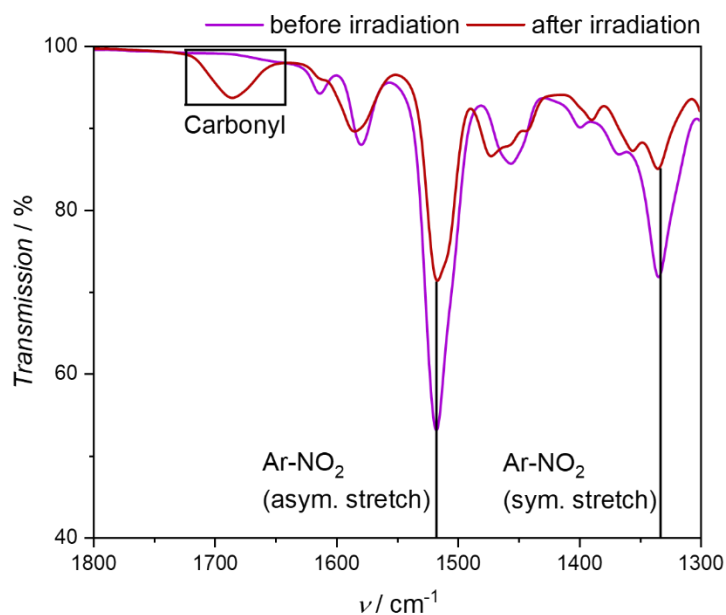


Figure S16: IR spectra before (purple) and after irradiation (red). The bars symbolize characteristic absorption bands and their decay during the irradiation process. Additionally, the black box symbolizes the rise of generated absorption bands. Irradiation parameters: 365 nm LED, 30 minutes, Acetonitrile-d₃.

2.3. Degradation of kinetics with LED irradiation

Maintaining the same distance between the sample and the LED ensures same irradiation conditions for the sample. Different LEDs were employed (**Figure S3**). After a set time, the sample is submitted to NMR spectroscopy, and afterwards exposed to further light. The conversion, X , is hereby calculated by

$$X_4 = \frac{I_4}{I_4 + I_{4'}}, X_{4'} = \frac{I_{4'}}{I_4 + I_{4'}} \quad \text{Eq. 1}$$

Table S5: Experimental parameters for the performed irradiation experiments. (*: performed in photovial to compensate UV absorption of ordinary glass).

LED	U / V	I / A	P_{calc} / W	dist / cm
340 nm*	0.44	4.4	1.94	2
365 nm	3.61	0.7	2.53	2
390 nm	3.70	0.61	2.26	2
415 nm	14.9	0.16	2.31	2

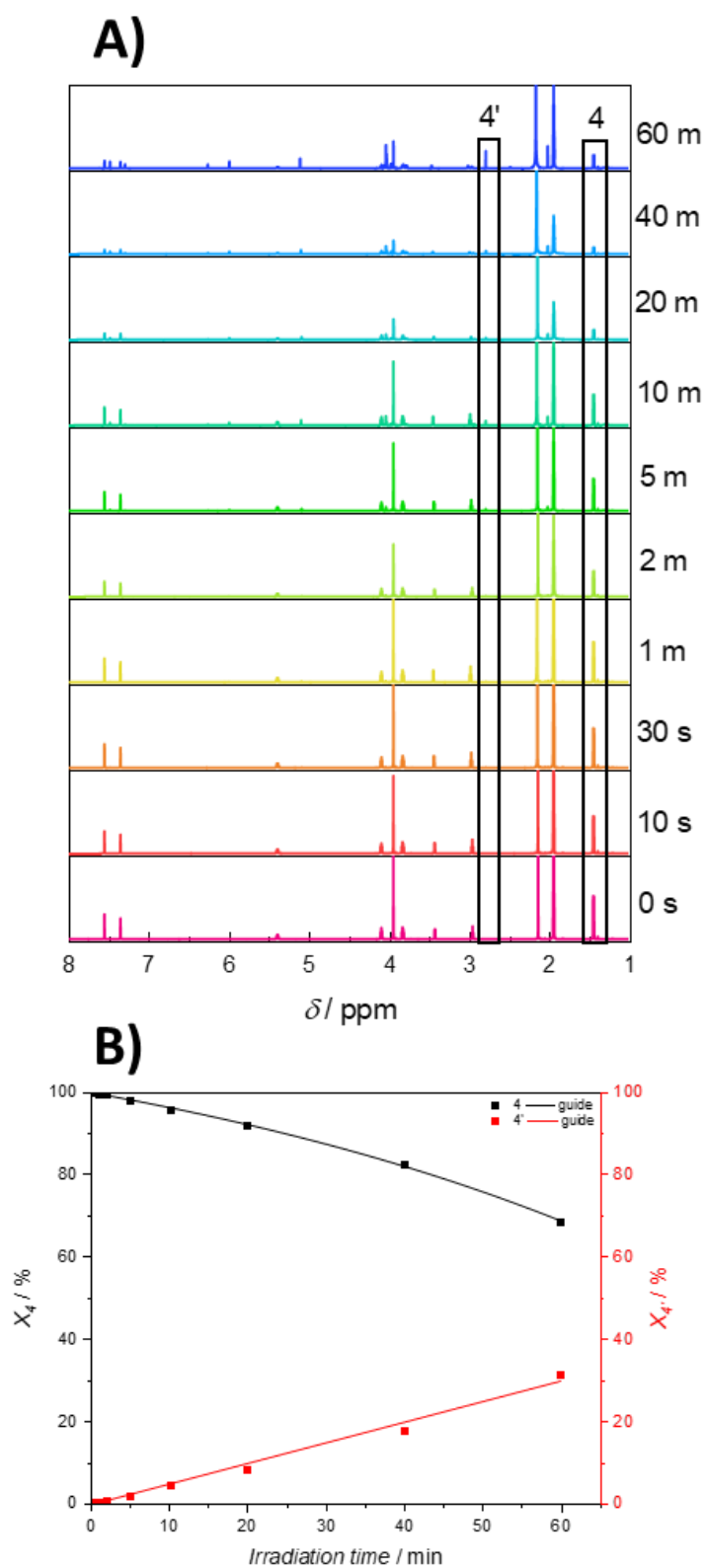


Figure S17: A) NMR spectra of **4** in DMSO- d_6 with 340 nm irradiation in different exposure times. B) Plot of conversion versus time for **4** (black) and **4'** (red).

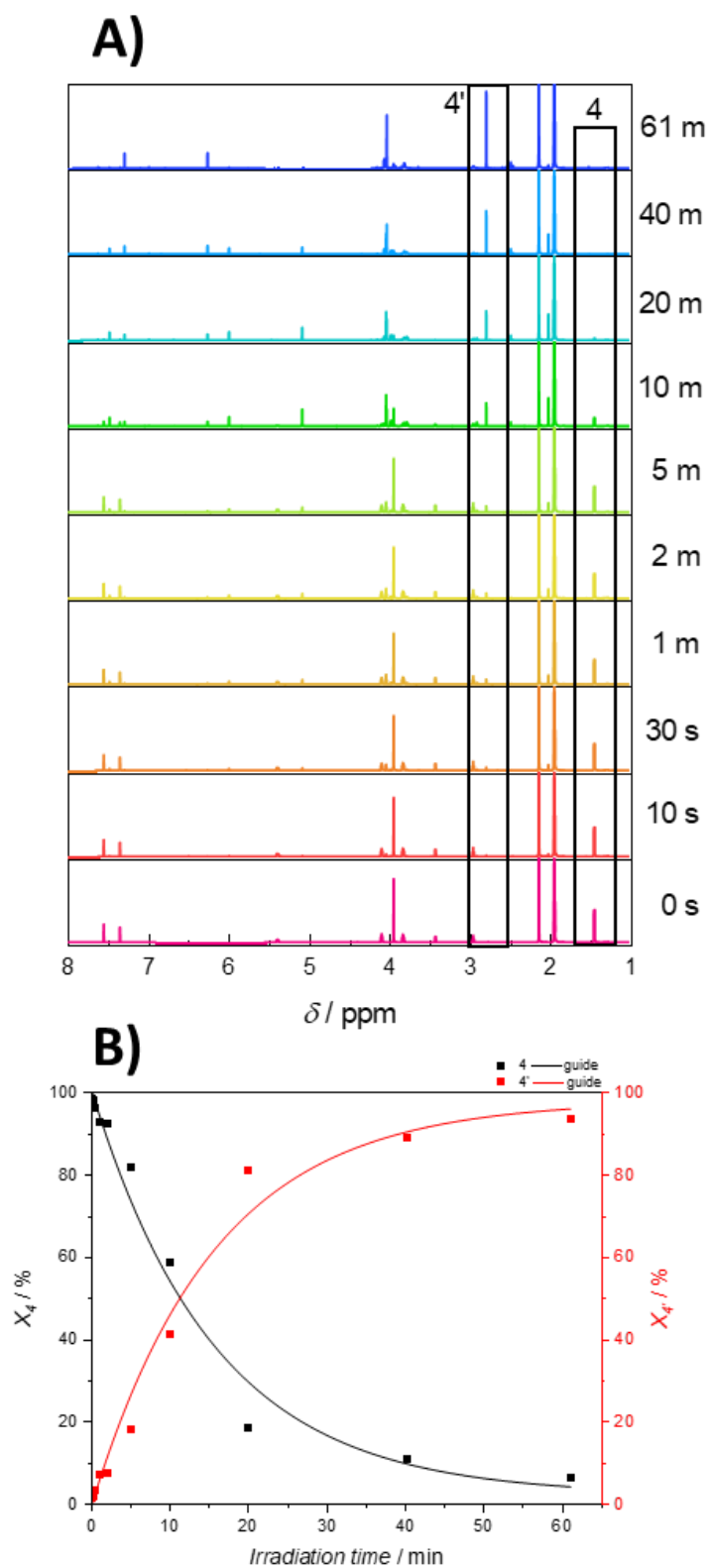


Figure S18: A) NMR spectra of **4** in DMSO-d₆ with 365 nm irradiation in different exposure times. B) Plot of conversion versus time for **4** (black) and **4'** (red).

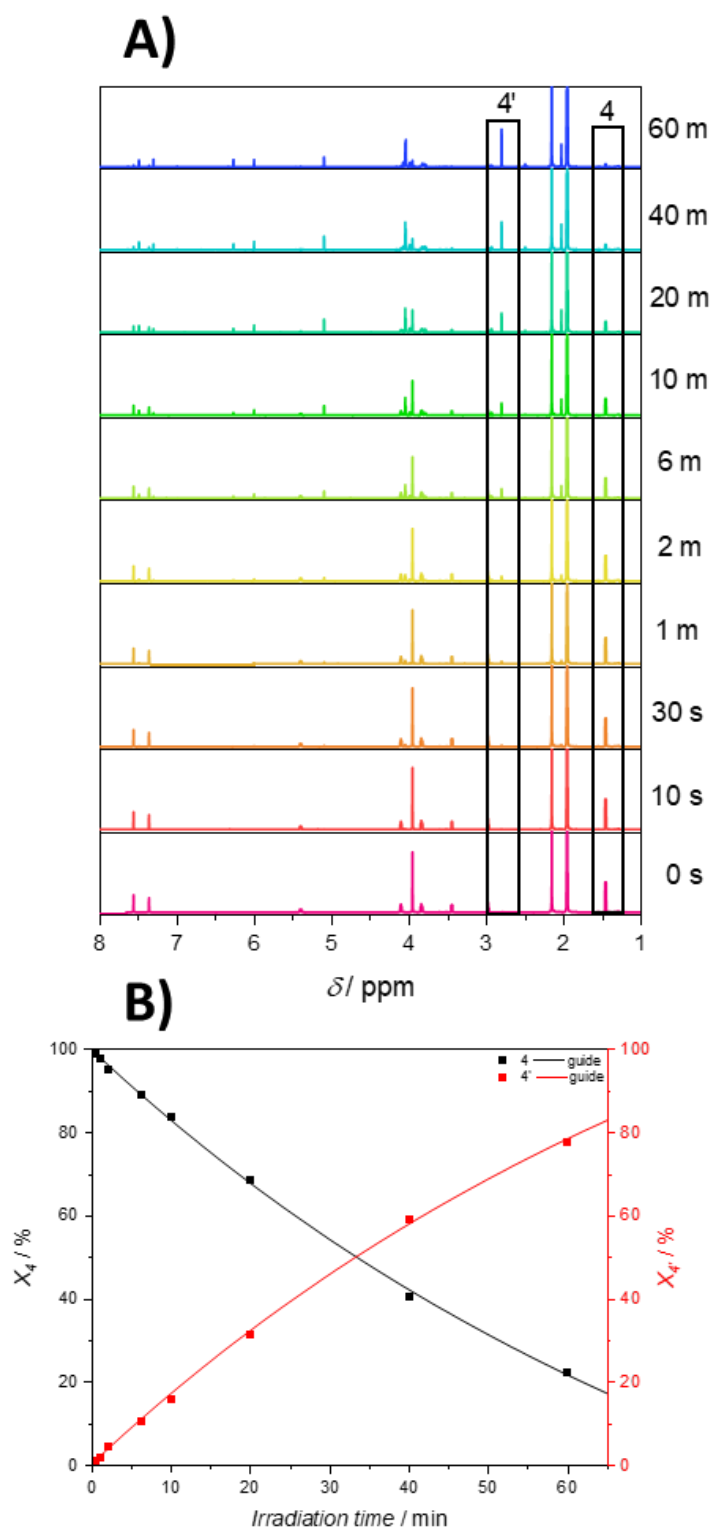


Figure S19: A) NMR spectra of **4** in DMSO- d_6 with 390 nm irradiation in different exposure times. B) Plot of conversion versus time for **4** (black) and **4'** (red).

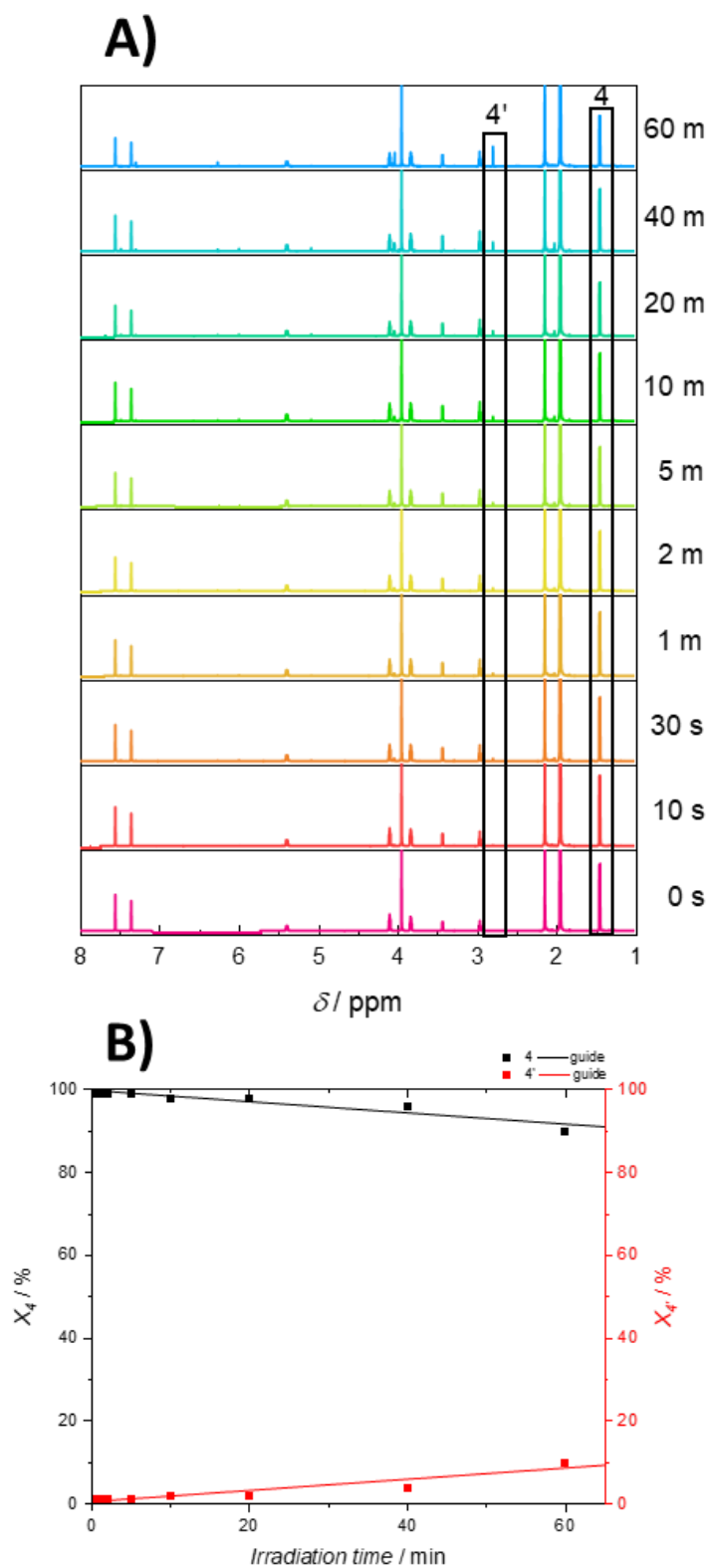
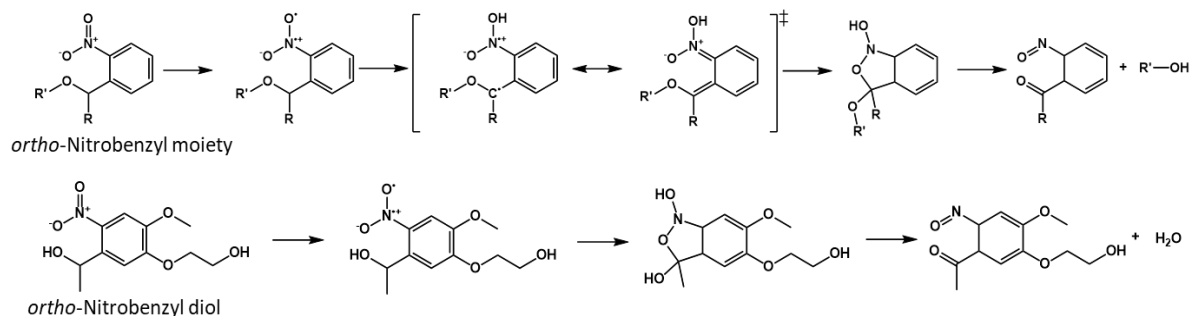


Figure S20: A) NMR spectra of **4** in DMSO-d₆ with 415 nm irradiation in different exposure times. B) Plot of Conversion versus time for **4** (black) and **4'** (red).

2.4. EPR of 4 under light irradiation



Scheme S3. Photolysis schemes of an ordinary *o*NB moiety (top) and of the *o*NB dialcohol, 4 (bottom).

Radical formation according to the in **Scheme S3** depicted mechanism was tracked via EPR. The degassed sample in α Acetonitrile- d_3 was irradiated with a 395 nm laser pointed into the sample holder and EPR spectra were recorded. Experimental settings are listed in **Table S6**.

Table S6: Settings for the recorded EPR spectrum.

Setting	Value
B_0 (center of magnetic field) / mT	336.5
R (range) / mT	5
t_{acq} (acquisition time) / s	60
N_R (Number of repetitions)	2
Gn (Gain mantisse)	7
Ge (Gain exponent)	2

The EPR spectrum was then simulated with the *garlic* function of the EasySpin package. Here, a given electron spin is simulated to couple with adjacent nuclei. The nature of the nuclei can

be set. Two systems were found, one with the electron being localized at the nitrogen nucleus and coupling with the nitrogen and two hydrogen (N3) nuclei and the other being located at a carbon and coupling with this carbon nucleus only (C1). Two spectra were convoluted representing the experimental spectrum. Simulation parameters are given in **Table S7**.

Table S7: Parameters obtained by the simulation of two radical species.

Parameters	N3	C1
g (gyromagnetic constant)	2.01766	2.01874
S (electron spin)	1/2	1/2
A (Hyperfine coupling constant) / MHz	[6, 22, 33]	[33]
lw (line width) / MHz	0.24	0.18
Abundance	56	1

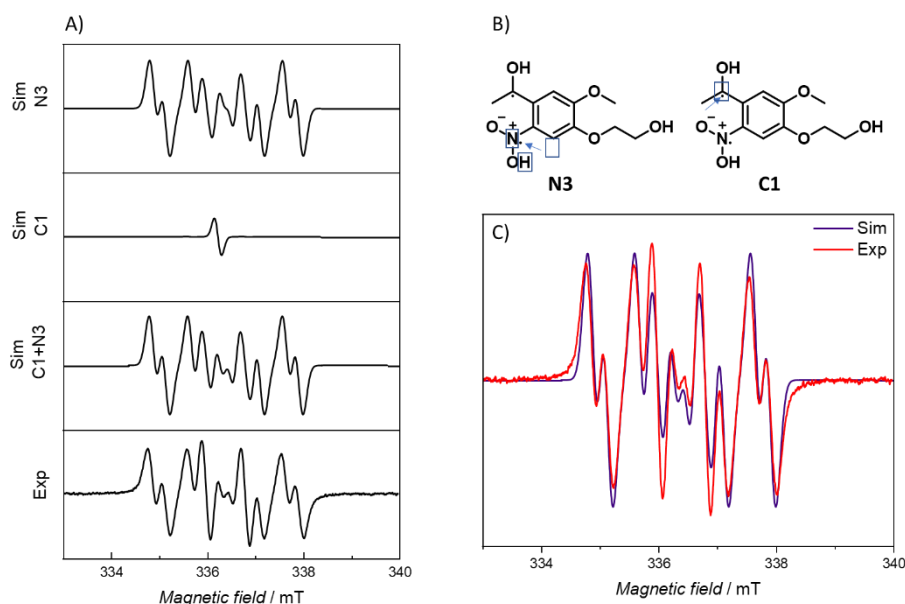


Figure S21: A) Extracted simulated spectra of N3, C1, the convolution of C1 and N3 and the experimental spectrum (from top to bottom). B) Assumed coupling pattern for the systems N3 (left) and C1 (right). The arrow indicates position of the radical, boxes represent coupling nuclei. C) Superimposed simulated and experimental spectra.

2.5. Action Plot of 4

Experiments were conducted in triplets (350 nm only twice). ¹H-NMR spectra were recorded in high-resolution (128 scans instead of 16). By setting the integral of the internal standard to 100, the integrals of **4** and **4'**, assigned to a and b (**Figure S15**) can be compared. The conversion *X* and Yield *Y* can then be calculated according to eq. 1 and 2.

Table S8: Parameters for the Action-Plot experiment. *: When conversion is determined to <0, resolution limit of the NMR spectrometer is assumed.

Entry	$n_p /$ μmol	$\Delta n_p /$ μmol	I_{IS}	I_4	$I_{4'}$	X_4	ΔX_4	$Y_{4'}$	$\Delta Y_{4'}$
300-1			100	69.20	12.83				
300-2	0.961	0.130	100	69.60	12.06	0.20147	0.00644	0.14171	0.00465
300-3			100	70.31	12.22				
310-1			100	67.49	14.20				
310-2	0.961	0.062	100	67.56	13.38	0.22202	0.00765	0.15783	0.00470
310-3			100	68.68	13.75				
320-1			100	70.23	12.33				
320-2	0.948	0.054	100	69.79	12.69	0.19571	0.00465	0.13766	0.01000
320-3			100	70.6	11.03				
330-1			100	72.22	10.71				
330-2	0.959	0.057	100	71.51	10.34	0.17386	0.00639	0.12395	0.00623
330-3			100	72.61	11.41				
340-1			100	72.6	9.78				
340-2	0.979	0.051	100	71.84	10.02	0.17463	0.00555	0.11429	0.00205
340-3			100	71.7	10.13				
350-1			100	74.14	9.84				
350-2	0.960	0.049	100	73.82	9.55	0.15248	0.00259	0.11107	0.00235
360-1			100	74.62	9.63				
360-2	0.953	0.059	100	75.61	8.41	0.14538	0.01169	0.10207	0.00732
360-3			100	73.57	8.69				
370-1			100	74.37	9.17				
370-2	0.958	0.056	100	75.95	8.54	0.14144	0.01002	0.10173	0.00364
370-3			100	74.51	8.93				
380-1			100	76.52	7.28				
380-2	0.969	0.082	100	75.45	7.36	0.13037	0.00631	0.08497	0.00197

380-3			100	75.76	7.61				
390-1			100	76.28	6.88				
390-2	0.972	0.088	100	76.41	7.02	0.12472	0.00138	0.07882	0.00160
390-3			100	76.52	6.74				
400-1			100	79.05	6.11				
400-2	0.960	0.083	100	79.15	5.87	0.09390	0.00059	0.06858	0.00138
400-3			100	79.08	5.98				
410-1			100	82.17	3.6				
410-2	0.960	0.058	100	81.96	3.69	0.06450	0.00813	0.04147	0.00072
410-3			100	80.85	3.57				
420-1			100	86.53	1.54				
420-2	0.945	0.164	100	86.65	1.48	0.01142	0.00593	0.01734	0.00035
420-3			100	85.7	1.52				
430-1			100	88.09	0.4				
430-2	0.968	0.070	100	87.5	0.37	-0.00481*	0.00378	0.00435	0.00020
430-3			100	87.54	0.37				
440-1			100	80.84	0.09				
440-2	0.960	0.058	100	87.97	0.17	0.01466	0.05179	0.00153	0.00046
440-3			100	89.22	0.14				
450-1			100	88.26	0.09				
450-2	0.963	0.073	100	88.39	0.08	-0.01398*	0.00375	0.00080	0.00030
450-3			100	88.88	0.04				
No irradi- ation			100	87.29	0	-	-	-	-

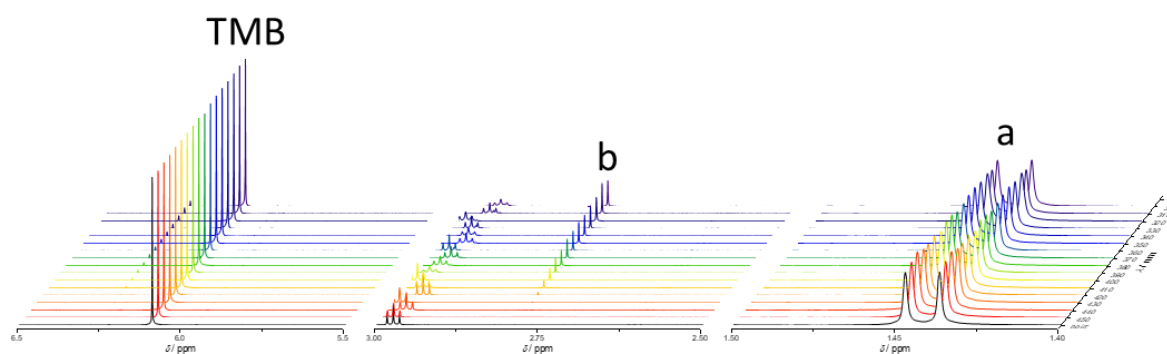


Figure S22: NMR spectra illustrating the analysis process. Due to simplicity, only the first entry of every wavelength is shown. By setting the integral of TMB to 100, the integrals of **4** and **4'** give access to the conversion in comparison to the non-irradiated sample (black).

2.6. Deconvolution of step-growth generated PU polymers

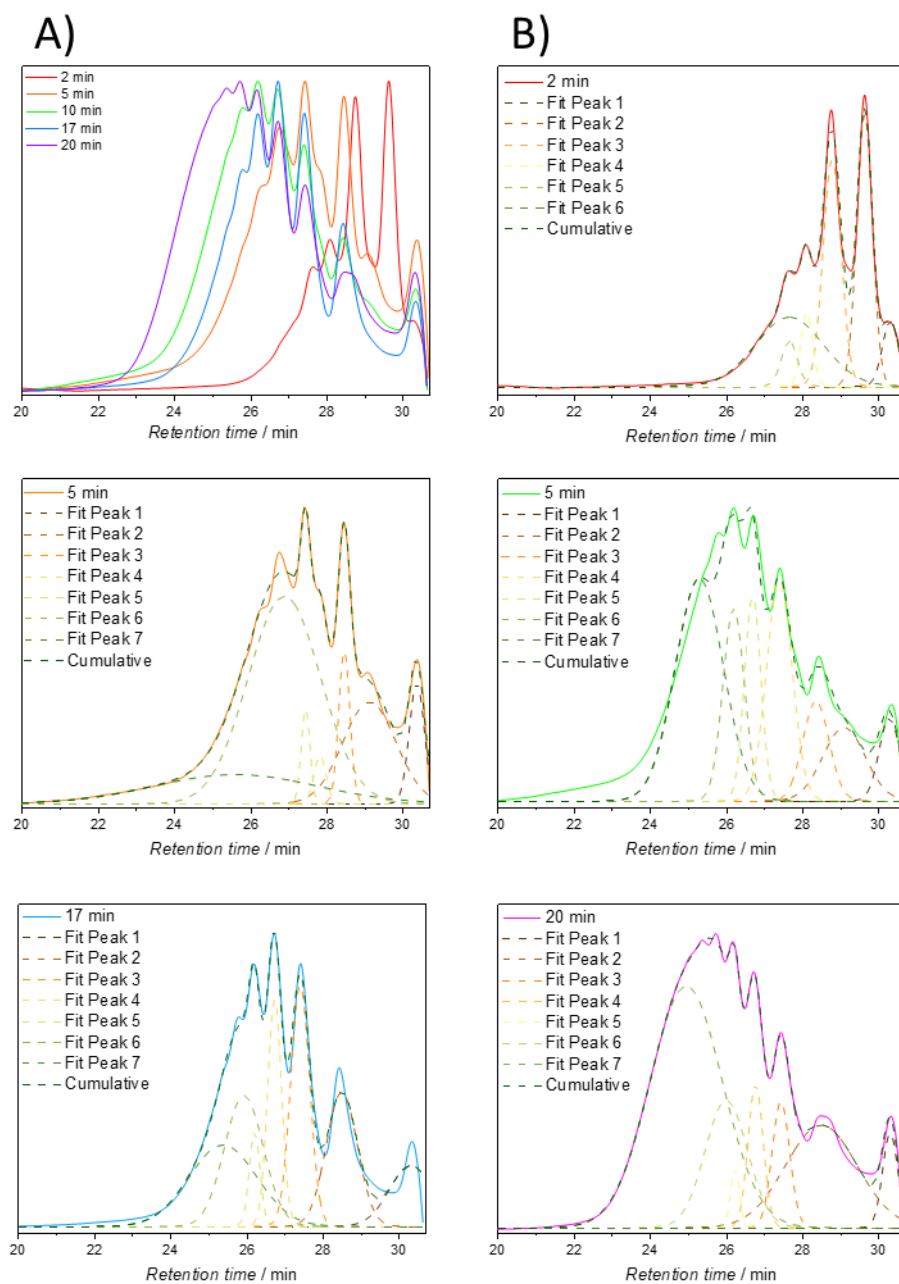


Figure S23: A) SEC traces (RI) of generated PUs. B) SEC traces of spectra (solid) and their deconvoluted Gaussians in dashed line.

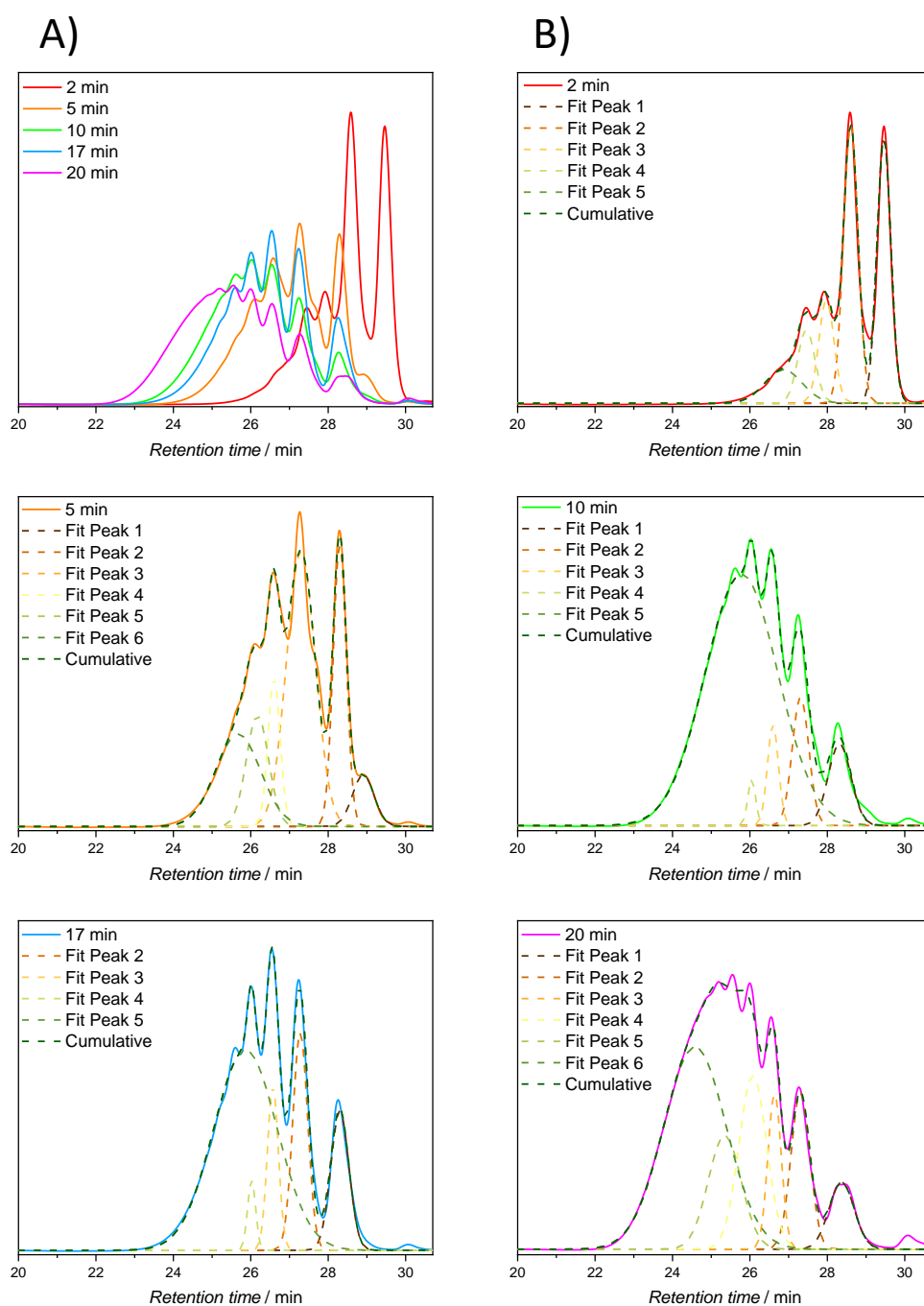


Figure S24: A) SEC traces (UV) of generated PUs. B) SEC traces of spectra (solid) and their deconvoluted Gaussians in dashed line.

2.7. PLD-SEC of step growth generated PU polymers

Assuming the *o*NB dialcohol, **4**, is incorporated as every second unit, the molar amount of *o*NB for a given mixture can be calculated easily. For every cured polymer (2 – 20 minutes), four

different exposure times (t1-t4) were selected. The equivalents of photons were then calculated on a case-to-case basis.

Table S9: Parameters for PLD-SEC experiments. Entry is given in (curing time)_(irradiation time)

Entry	λ / nm	E_{pulse} / μJ	ΔE_{pulse} / μJ	k	$T_c(\lambda)$	$N_A hc$ / J m mol^{-1}	n_P / μmol	Δn_P / μmol	n_{oNB} / μmol	eq. $h\nu$ vs. oNB	$\Delta \text{eq. } h\nu$ vs. oNB
2 min_t1	340	728	16.4	1500	79.8179	0.119705316	2.48	0.056	2.90	0.85	0.02
2 min_t2	340	736	17.6	3000	79.8179	0.119705316	5.01	0.120	2.96	1.69	0.04
2 min_t3	340	726	16.0	6000	79.8179	0.119705316	9.88	0.218	3.62	2.73	0.06
2 min_t4	340	733	16.2	12000	79.8179	0.119705316	19.94	0.441	3.23	6.18	0.14
5 min_t1	340	728	16.4	1500	79.8179	0.119705316	2.48	0.056	3.13	0.79	0.02
5 min_t2	340	736	17.6	3000	79.8179	0.119705316	5.01	0.120	3.00	1.67	0.04
5 min_t3	340	726	16.0	6000	79.8179	0.119705316	9.88	0.218	3.82	2.59	0.06
5 min_t4	340	733	16.2	12000	79.8179	0.119705316	19.94	0.441	3.32	6.00	0.13
10 min_t1	340	728	16.4	1500	79.8179	0.119705316	2.48	0.056	3.13	0.79	0.02
10 min_t2	340	736	17.6	3000	79.8179	0.119705316	5.01	0.120	4.11	1.22	0.03
10 min_t3	340	726	16.0	6000	79.8179	0.119705316	9.88	0.218	4.31	2.29	0.05
10 min_t4	340	733	16.2	12000	79.8179	0.119705316	19.94	0.441	3.26	6.12	0.14
17 min_t1	340	728	16.4	1500	79.8179	0.119705316	2.48	0.056	3.16	0.78	0.02
17 min_t2	340	736	17.6	3000	79.8179	0.119705316	5.01	0.120	3.03	1.65	0.04
17 min_t3	340	726	16.0	6000	79.8179	0.119705316	9.88	0.218	3.72	2.66	0.06
17 min_t4	340	733	16.2	12000	79.8179	0.119705316	19.94	0.441	3.36	5.94	0.13
20 min_t1	340	728	16.4	1500	79.8179	0.119705316	2.48	0.056	2.96	0.84	0.02
20 min_t2	340	736	17.6	3000	79.8179	0.119705316	5.01	0.120	3.59	1.40	0.03
20 min_t3	340	726	16.0	6000	79.8179	0.119705316	9.88	0.218	3.82	2.59	0.06
20 min_t4	340	733	16.2	12000	79.8179	0.119705316	19.94	0.441	3.49	5.72	0.13

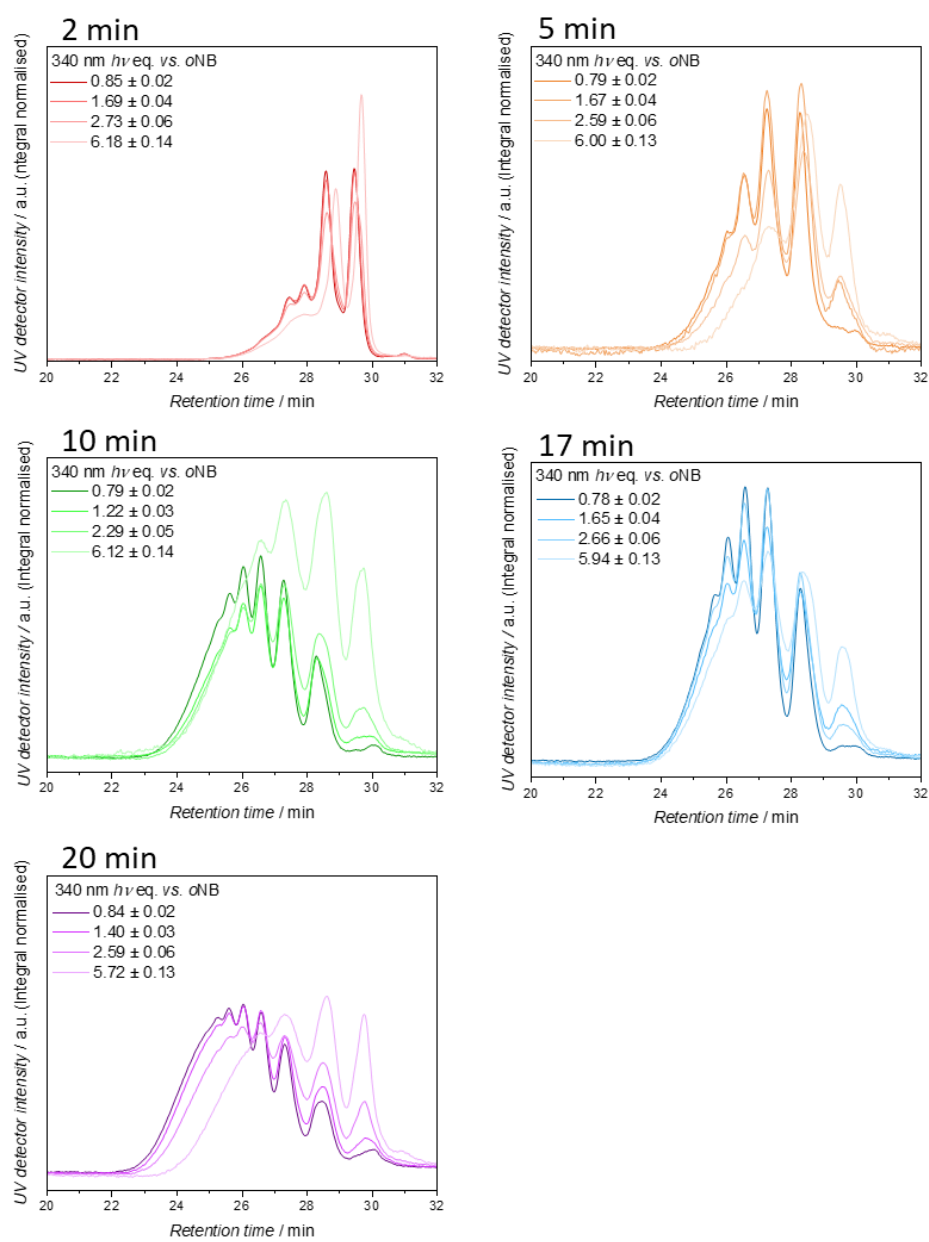
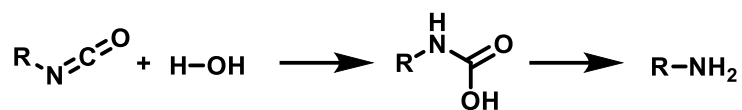


Figure S25: PLD-SEC experiments of the cured polymers in solution in THF.

2.8. SEC-ESI- MS of PUs



Scheme S4: Reaction scheme of isocyanate with water leading to the formation of an amine.

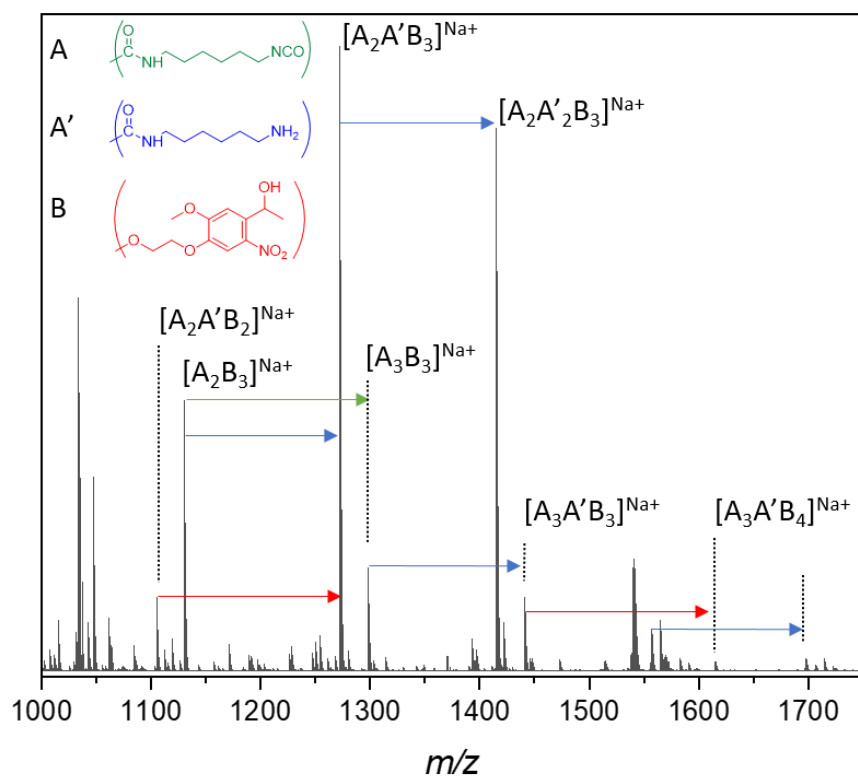


Figure S26: SEC-ESI MS spectra of poly(urethane-*o*NB) (20 min) averaged over retention times of single charged polymer from 18.8 to 20.6 min. The isocyanate unit (m/z 168.09) is displayed in green, the reduced isocyanate unit (m/z 142.11) in blue and the *o*NB unit (m/z 257.09) in red.

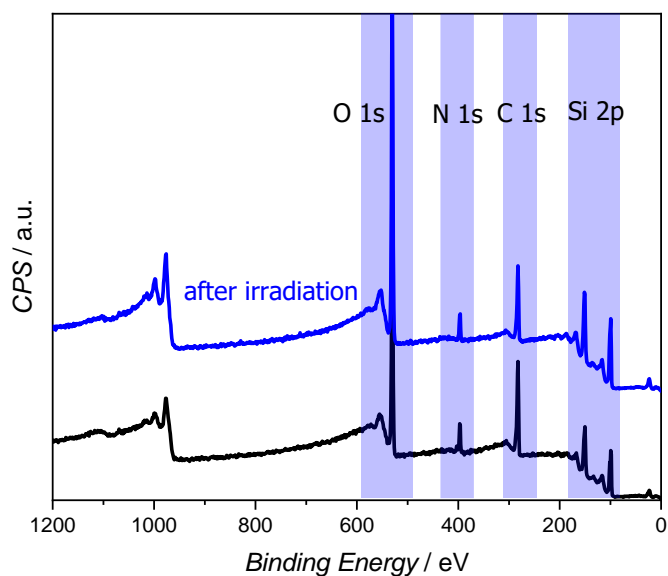


Figure S27: Wide scan XPS spectra of thin films of *o*NB-Polyurethane before (black) and after (blue) UV irradiation.

References

- [1] Gruending, T.; Guilhaus, M.; Barner-Kowollik, C. *Macromolecules* **2009**, *42*, 6366.
- [2] Stoll, S.; Schweiger, A. *J. Magn. Res.* **2006**, *178*, 42-55.
- [3] Marschner, D. E.; Frisch, H.; Offenloch, J. T.; Tuten, B. T.; Becer, C. R.; Walter, A.; Goldmann, A. S.; Tzvetkova, P.; Barner-Kowollik, C. *Macromolecules* **2018**, *51*, 3802-3807.
- [4] Kim, M. S.; Grunreich, J.; Jing, S.; Diamond, S. L. *J. Mater. Chem.* **2010**, *20*, 3396-3403.